



APPLICATION FOR OBSERVING TIME

LARGE PROGRAMME

PERIOD: **101A**

Important Notice:

By submitting this proposal, the PI takes full responsibility for the content of the proposal, in particular with regard to the names of CoIs and the agreement to act according to the ESO policy and regulations, should observing time be granted.

1. Title		Category: A-9							
RAMS: The Radio-AGN MUSE Survey: Determining the triggering and impact of a benchmark sample of powerful radio Active Galactic Nuclei.									
2. Abstract / Total Time Requested									
Total Amount of Time:		Total Number of Semesters:							
<p>Active Galactic Nuclei (AGNs) are believed to regulate galaxy growth by injecting vast amounts of energy into their host galaxies and halos which shuts-off star formation. This “AGN feedback” is supported by observations of powerful outflows launched from AGNs into their immediate surroundings. However, we still do not know how AGNs are triggered, nor what drives their outflows. This raises major uncertainties regarding whether AGN feedback is accurately implemented in models of galaxy evolution. To address this requires mapping the kinematics of AGN outflows and host galaxies at high spatial resolutions, which can only be achieved via IFU observations of nearby AGNs. To date, all IFU surveys of nearby AGNs have focussed on radio-weak AGNs, yet there is strong evidence that radio-powerful AGNs play a major role in driving feedback-inducing outflows. It is likely, therefore, that IFU surveys of AGNs have so far ignored one of the most important drivers of AGN feedback. We propose to address this by using MUSE to conduct the first IFU survey of a representative sample of local, radio-powerful AGN. From this, we will determine (a) how powerful radio AGNs are triggered; (b) the role of radio jets vs. radiative driving in powering feedback-inducing AGN outflows; and (c) the mass/momentum/energy content of these outflows, and whether they have a significant impact on their host galaxies.</p>									
3. Run	Period	Instrument	Time	Month	Moon	Seeing	Sky	Mode	Type
A	101	MUSE	33.1h	any	g	1.0	PHO	s	
B	102	MUSE	21.7h	any	g	1.0	PHO	s	
C	103	MUSE	34.1h	any	g	1.0	PHO	s	
D	104	MUSE	21.7h	any	g	1.0	PHO	s	
4. Principal Investigator: jmulaney									
4a. Co-investigators:									
C.	Tadhunter		1245						
D.	Alexander		1237						
E.	Bernhard		1245						
P.	Bessiere		1824						
D.	Dicken		1193						
C.	Harrison		1258						
<i>Following CoIs moved to the end of the document ...</i>									

5. Description of the proposed programme

A – Scientific Rationale:

The case for AGN feedback: Determining how today’s galaxies have grown and evolved to their present state is the primary goal of extragalactic research. It is now clear that galaxy growth is strongly regulated by so-called “feedback” processes (e.g., Vogelsberger et al. 2014, Schaye et al. 2015). Among the most important of these is the suppression of galaxy growth by Active Galactic Nuclei (AGNs) that heat and/or expel gas which would otherwise collapse to form stars (see Fabian, 2012; Harrison, 2017 for reviews). Without this “AGN feedback”, models of galaxy growth fail to reproduce the masses, shapes and sizes of the observed galaxy population. As such, **it is widely considered that AGNs have played a major role in shaping today’s galaxies.**

Recently, models invoking AGN feedback have received significant empirical support from observations. Firstly, X-ray observations of nearby clusters have revealed AGNs injecting considerable amounts of energy into the intergalactic medium, preventing it from cooling and forming stars (e.g., McNamara & Nulsen 2012). Secondly, there is clear evidence of fast (i.e., $> 500 \text{ km s}^{-1}$), ionised outflows in the optical and near-infrared spectra of a significant fraction (i.e., $\sim 20\%$; e.g., Mullaney et al. 2013; Harrison et al. 2014) of all AGNs. Both provide strong evidence of energy transport from AGNs, as required by feedback models. The problem we face, however, is that we do still not understand (a) how AGNs are triggered and (b) what mechanism drives the outflows that transport energy from the AGN. Until these questions are addressed, it will remain impossible to test whether AGN feedback is being accurately implemented in models of galaxy growth.

The role of IFU surveys in studies of AGN feedback: The key to determining how AGNs are triggered are spatially resolved kinematics of their host galaxies. This is because any triggering mechanism must funnel gas to fuel the AGN from galactic scales to the nucleus. Similarly, to determine how AGN outflows are driven requires spatially resolved observations of those outflows, mapped-out by their gas kinematics. Such spatially resolved kinematics of the outflows and, in particular, the host galaxy can *only* be delivered by integral field (IFU) observations of *low redshift* (i.e., $z < 0.4$) AGNs. Further, since AGNs and their host galaxies display a lot of diversity, it is important to conduct IFU surveys of sufficient numbers of AGNs to identify underlying trends with, e.g., luminosity, mass, host morphology etc.

To date, the only large IFU survey of nearby AGNs has focussed radio-weak AGNs (i.e., CARS [PI: Husemann]). However, **there is strong evidence of an association between fast, ionised outflows and radio-powerful AGNs**, with 50% of AGNs with 1.4 GHz radio luminosities ($L_{1.4\text{GHz}}$) above $10^{23} \text{ W Hz}^{-1}$ displaying evidence of powerful ($> 500 \text{ km s}^{-1}$) outflows, compared to just 10% of those below this radio luminosity threshold (Mullaney et al. 2013; Fig. 1, *left*). Furthermore, our own resolved long-slit and IFU observations of nearby radio AGNs show clear signs of interaction between radio jets and the ISM (e.g., Holt et al. 2008, Tadhunter et al. 2014, Santoro et al. 2015). This raises the prospect that jets launched from radio AGNs are an important driver of powerful gas outflows, as predicted by the hydrodynamical simulations of jet/gas interactions described in Wagner et al. (2011; Fig. 1 *right*; also Mukherjee et al. 2016). Furthermore, radio loud AGNs are the *only* type capable of inducing “radio-mode” AGN feedback, which is thought to heat intergalactic gas, preventing it from collapsing onto galaxies to form stars (e.g., Bower et al. 2006). Since radio powerful AGNs have largely been avoided by IFU surveys, it is likely that they have ignored one of the most important drivers of AGN feedback. The focus of our proposal is to address this by using MUSE to conduct the first IFU survey of a representative sample of local, radio-powerful AGNs.

B – Immediate Objective: We will use the MUSE IFU to obtain deep spectral coverage of the host galaxies of a representative sample of powerful radio AGNs in the local Universe. **With these observations, we will determine (a) how powerful radio AGNs are triggered; (b) the role of jets vs. radiative driving in powering AGN outflows; and (c) the mass/momentum/energy content of these outflows, and whether they have a significant impact on their host galaxies.**

The Sample

Our target sample is selected from the **2 Jy sample** of radio powerful AGNs, originally described in Wall & Peacock (1985). The original 2 Jy sample contains all sources with 2.7 GHz fluxes above 2 Jy, although we select only the southern sample, defined as having declinations below $+10^\circ$. This represents a total of 88 objects, although 42 of these have strongly beamed emission along our line of sight and are not suitable for studies of the host galaxy or resolved outflows. This leaves a sample of 46 non-beamed, southern 2 Jy sources. From these 46, we select only those 36 at $z < 0.4$ (hereafter, “our sample”). These 36 radio AGNs span the radio luminosity range: $25.0 < \log(L_{5\text{GHz}}/\text{W Hz}^{-1}) < 27.4$. They represent the full diversity of radio AGNs: 36% are broad line (i.e., Type 1) AGNs or quasars, 42% are narrow-line (i.e., Type 2) AGNs, while the remaining 22% are weak-line radio AGNs associated with low AGN accretion rates, yet still display powerful radio jets (Tadhunter et al. 1993). Their diversity in class and luminosity means it is important that we observe the full sample to obtain statistically meaningful numbers of AGNs in important class and luminosity bins. Over the past two decades, our team has led numerous campaigns to obtain extensive coverage of the southern 2 Jy sample across the full observable electromagnetic spectrum. The 2Jy is unique in terms of the completeness

5. Description of the proposed programme (continued)

of its multi-wavelength data that includes X-ray imaging/spectroscopy (*Chandra*, XMM), optical spectroscopy (ESO 3.6m & VLT), optical imaging (*Gemini*), near-IR imaging (ESO NTT & VLT), mid to far-IR photometry (*Spitzer* & *Herschel*), mid-IR spectroscopy (*Spitzer*) and radio imaging (VLA and ATCA); *it is now the best observed of any sample of radio-loud AGN. The 2 Jy sample therefore represents our best possible opportunity to determine what processes trigger powerful radio AGNs and drive their outflows.*

The Observations

In this section we highlight how our MUSE observations of the 2 Jy sample will build upon our current understanding of radio AGNs, enabling us to determine how radio AGNs are triggered, how their outflows are driven, and measure the properties and impact of these outflows.

How are radio AGNs triggered?: To establish what triggers radio AGNs demands detailed observations of their immediate surroundings, and in particular their host galaxies. Initial inspection reveals that the majority of radio AGNs reside in massive ($> 10^{11} M_{\odot}$), early type galaxies (e.g., Matthews, Morgan & Schmidt 1964). However, our own detailed morphological studies of the 2 Jy sample have revealed that features such as tidal tails, fans, shells, and bridges occur far more frequently around powerful radio AGNs compared to luminosity-matched comparison early-type galaxies (94% of radio AGNs vs 50% of non-active early-types when of similar surface brightness; Ramos Almeida et al. 2011, 2012; Fig. 2). This indicates a far more violent *recent* merger history than their early-type morphologies initially suggest.

The prevalence of tidal features around radio AGNs provides clear evidence that galaxy interactions play a role in triggering at least some powerful radio AGNs. However, with both major and minor mergers capable of producing strong tidal features, it is not clear what type of merger trigger radio AGN. Thankfully, stellar kinematics can be used to distinguish between the types of mergers that have taken place. Fast rotating early-type galaxies are produced by wet, major mergers, while slow rotators are thought to be produced by dry major or a series of minor mergers (Cappellari et al. 2016 and references therein).

To date, only a handful of radio AGNs have had their hosts' stellar kinematics measured, and even then only with long-slit spectra out to only a fraction of an effective radius (Smith and Heckman et al. 1990, Bettoni et al. 2001). These few shallow observations provide tantalising, yet unconfirmed, evidence that radio AGNs are associated with fast rotators. If confirmed, this would connect powerful radio AGNs to major wet mergers, possibly representing a post-starburst phase, since local Ultra Luminous Infrared Galaxies (ULIRGs) are also associated with fast rotation (e.g., Genzel et al. 2001; Tacconi et al. 2002). Should they instead be triggered by an alternative mechanism, such as accretion of hot halo gas or minor mergers as suggested by some models (e.g., King & Pringle 2006; Hopkins & Quataert 2010), they would show a preference toward slowly-rotating early-type galaxies. Finally, should radio AGNs show no preference to either fast or slow rotators, it would imply that the type of merger is not important, with either wet, dry, major or minor capable of triggering them.

By mapping the stellar kinematics across the entire host galaxy, our MUSE observations will determine what type of galaxy interaction are required to trigger powerful radio AGNs.

With our MUSE observations, we will spatially resolve (to at least one effective radius) the host galaxies of all our sample. We will measure the off-nuclear stellar velocity shift (V) and velocity dispersion (σ) from stellar absorption lines. At the low redshifts of these sources, the MUSE spectra will cover the strong $\text{Mg}\lambda 5200$ absorption line, although we will fit the whole stellar continuum with gaussian-convolved stellar templates to maximise the information from the stellar continuum (i.e., excluding emission lines and using the Penalised Pixel-Fitting method of Cappellari & Emsellem, 2004). To extract just the first two velocity modes (i.e., V and σ) requires a comparatively low continuum signal-to-noise of ~ 10 (e.g., Cappellari et al. 2007). To ensure we measure the characteristic kinematics of the whole galaxy, rather than just the core, *it is vital that we reach this sensitivity to at least one effective radius* (a diameter of 20 kpc, or $20''$ [$4''$] for our lowest [highest] redshift target). This can only be achieved with deep (~ 2 hr) observations (see Box 9).

We will use the criteria of Emsellem et al. (2007) to distinguish between fast and slow rotating early type radio AGN hosts. This uses the resolved V and σ maps to overcome some of the degeneracies associated with traditional V/σ measurements. Next, we will compare the relative numbers of fast and slow rotators in our sample against mass-matched samples of non-AGN early type galaxies from the ATLAS^{3D} survey (Cappellari et al. 2011). Should our sample display a significant departure from the relative numbers of fast to slow rotators in this comparison sample, it would imply a preference of one over the other. We will also compare against the radio-weak AGNs targeted with MUSE as part of the Close AGN Reference Survey (CARS; PI: Husemann) to determine whether powerful radio AGNs show evidence of being triggered via different mechanisms compared to radio-weak AGNs. With 36 radio AGNs, our sample contains sufficient statistics to robustly test for this as a function of AGN type (broad line, narrow line, weak line) and luminosity, thereby demonstrating whether different classes of AGNs are triggered by different mechanisms.

What drives outflows from radio AGNs?: To have any impact on galaxy evolution, the energy from an AGN, radio powerful or otherwise, must be transmitted into their host galaxies or surrounding material *and* effect some influence. Our team has played a leading role in identifying fast, yet non-relativistic ($\sim 1000 \text{ km s}^{-1}$) winds associated with powerful AGNs (e.g., Tadhunter et al. 2001, 2014; Alexander et al. 2008; Villar-Martin

5. Description of the proposed programme (continued)

et al. 2014, 2016; Harrison et al. 2014; Santoro et al. 2015; Spence et al. 2016; Figs. 3 & 4). These winds are often extended over kpc-scales, thereby *potentially* affecting a large fraction of the host galaxy as demanded by AGN feedback models (e.g., Alexander et al. 2008; Harrison et al. 2012, 2014; Tadhunter et al. 2014). Our investigations have also found that such winds are more prevalent among AGNs displaying evidence of nuclear radio emission. Indeed, our long-slit observations of a subsample of the 2 Jy sample has shown that some of the fastest AGN winds in the local Universe are associated with powerful radio AGNs (e.g., Tadhunter et al. 2016). As such, it is important for our models of feedback that we establish their primary driving mechanism, whether the radio jet or the intense radiation from the AGN. **Our MUSE observations will achieve this by mapping the winds in the 2 Jy AGN, allowing us to relate them to the resolved radio jets.**

By measuring the profiles of the strong forbidden [O III] λ 5007 emission line, we will map the kinematics of the ionised gas in our sample. The [O III] line traces low density gas and has been used extensively in recent studies, not least our own, to successfully measure the kinematics and extent of outflows in AGN host galaxies. The ionised phase, however, only represents a fraction of the gas in a galaxy, so we will use the Na I $\lambda\lambda$ 5890, 5896 absorption lines to map the kinematics of the neutral gas phase (e.g., Rupke & Veilleux, 2013). *It is important that we have sufficiently deep observations to measure this absorption line against the stellar continuum.* Any Na I absorption intrinsic to the stellar continuum will be modelled using stellar templates. At every position in the galaxy, we will decompose the [O III] and Na I lines into their various kinematic components, identifying those regions displaying the strongly shifted or broad kinematic components characteristic of powerful AGN outflows. By mapping the stellar and gas kinematics across the whole galaxy, *our deep observations will be able to identify even small departures from gravitational motions, and thus be highly sensitive to extended outflows.* We will then relate the location of the outflows to the positions of the radio jets that have already been mapped-out at high (i.e., sub-arcsecond) resolutions with our VLA and ATCA observations. *Should any AGN show outflows with a significantly wider opening angle than the jets, it would imply radiative driving in that case.*

What effect do AGN outflows have on their host galaxies?: As well as establishing the mechanism driving AGN winds, to test AGN feedback models we must also determine whether they have any real effect on their host galaxies. The first step in doing this is to measure the energy content of the wind and (i) compare it to model predictions and (ii) empirically assess whether it is sufficient to evacuate the galaxy of significant fraction of its gas content. The second step is to determine whether the winds are having a direct influence on the host by comparing the rates of star formation within the winds against those in the rest of the galaxy. All of the 2 Jy sample have *Spitzer* and *Herschel* coverage, providing obscuration-independent star formation rates (SFRs). However, the host is only resolved at these infrared wavelengths in a small minority of cases. For the others, we will use the MUSE spectra to produce resolved BPT diagnostics to map-out regions of star-formation within the host galaxies and, following e.g., Perna et al. (2015) & Maiolino et al. (2017), relate these regions to the resolved AGN outflows. **By mapping the source of ionising radiation (AGN, star formation), and density and kinematics of the outflows, our MUSE observations will provide the information needed to comprehensively measure the impact of radio AGNs on their host galaxies.**

To measure the energy content of the extended outflows requires knowledge of their mass content. Thirty-five of our sample are at low enough redshifts that the [S II] $\lambda\lambda$ 6717, 6732 doublet falls within the spectral range of MUSE, enabling us to use this density-sensitive line for mass measurements. This density information, combined with the kinematics and extents of the outflows, will enable us to determine the mass and mass flux of the outflows. From this, we will measure the energy and momentum content of the outflows. This will be compared against model predictions (e.g., Zubovas & King 2012; Gabor & Bournaud 2014) and the gravitational potential of the galaxy (measured from stellar and non-outflowing gas kinematics) to determine whether the outflows contain sufficient energy to have a significant impact on host.

Finally, we will use the approach of using resolved BPT diagnostics outlined in e.g., Perna et al. (2015); Maiolino et al. (2017) to directly measure the impact of the outflows on star formation within the extended outflows. This method solves the problem that the H β , [O III] λ 5007, [O III] $\lambda\lambda$ 6548, 6584 and H α lines (i.e., the traditional emission lines used in BPT diagnostics) are dominated by AGN ionisation by kinematically decomposing the emission lines into separate AGN-ionised and star formation-ionised components. By relating regions of star-formation to the locations of the outflows, we will measure the impact of these outflows on star formation within the host galaxy (whether they enhance [positive feedback] or suppress [negative feedback] star-formation). Since BPT diagnostics are sensitive to star formation within the past ~ 10 Myr, this provides a measurement of the immediate effect of AGN feedback (whether positive or negative) on short timescales before the AGN has had a chance to “switch off” (e.g., Hickox et al. 2014)

C – Telescope Justification: MUSE is the only IFU available to us that has the sensitivity and field-of-view needed to achieve our immediate science goals.

D – Observing Mode Justification (visitor or service): As we are applying to use MUSE in a standard setup, service mode is more suitable as it guarantees our requested observing conditions.

5. Attachments (Figures)

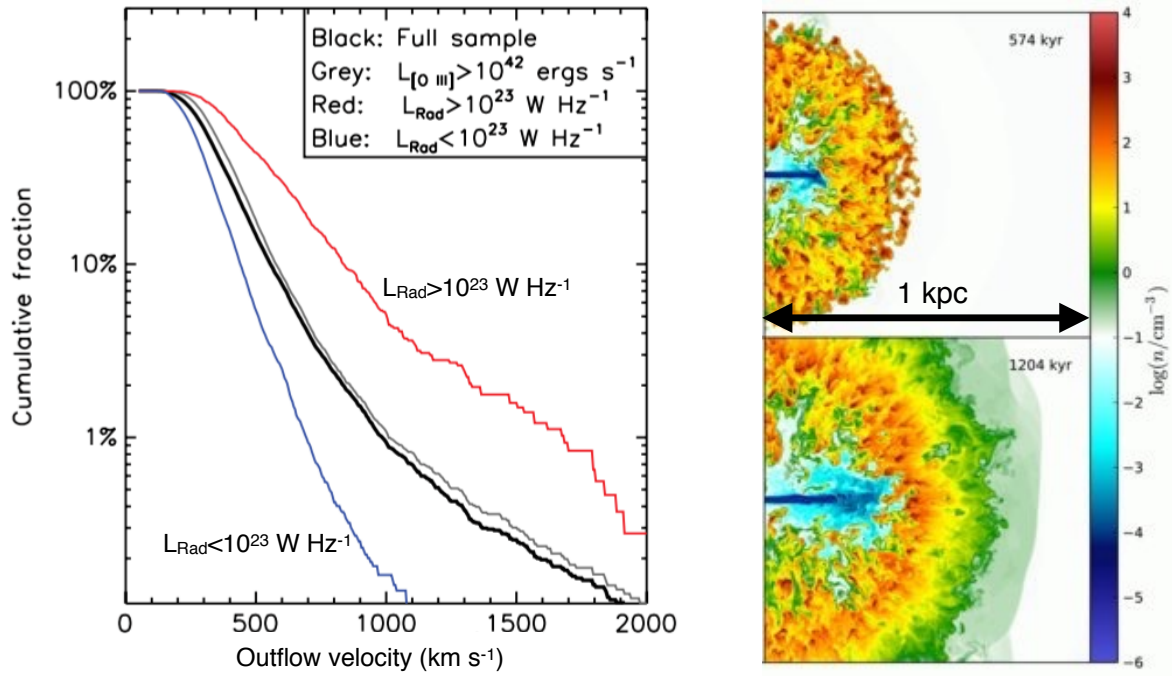


Fig. 1 *Left*: The fraction of emission line-selected AGNs in the SDSS at $z < 0.4$ with (unresolved) outflow velocities greater than the value shown on the x-axis (from Mullaney et al. 2013). Outflow velocities are measured from the profile of the [O III]5007 emission line. The sample has been split according to radio luminosity and [O III] luminosity (see labels). A much higher fraction of powerful radio AGNs display evidence of fast outflows compared to low radio luminosity AGNs. This indicates that radio luminous AGNs are more capable of driving outflows, yet most AGN IFU surveys have focussed on radio-weak AGNs. *Right*: Simulated interaction between an AGN-launched radio jet and the interstellar material, 500kyr and 1.2 Myr after jet onset (from Wagner et al. 2011). These hydrodynamical simulations demonstrate the capability of radio jets in disrupting dense gas within the host galaxy. Our MUSE observations will map-out the kinematics of the outflows in radio AGN to determine whether they are, indeed, jet driven.

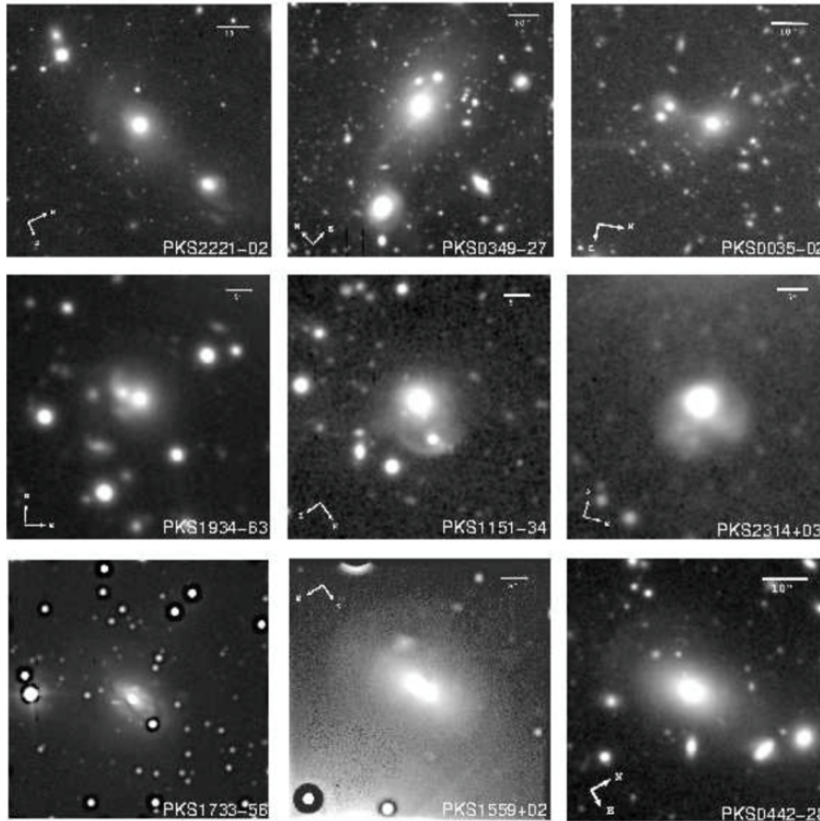


Fig. 2 Examples of deep optical r-band images of 2 Jy radio galaxies from Ramos Almeida et al. (2011). The angular scale is shown by the white line in the upper right of each panel which is 5'' long. While all are hosted in early-type galaxies, they display significant diversity in their detailed structures. While PKS2221-02, PKS0349-27, PKS0035-02, PKS1934-63 and PKS1151-34 are pre-coalescence systems that show evidence for tidal interactions with neighbouring galaxies, PKS2314+03, PKS1733-56, PKS1559+02 and PKS0442-28 are post-coalescence systems that show evidence for high surface brightness tidal features (PKS2314+03, PKS1733-56) or more subtle shell structures (PKS1559+02, PKS0442-28). These complex structures indicate that radio galaxies have a far more violent recent merger history than their early-type morphologies initially suggest. However, it is not clear what types of interactions are most likely to trigger a radio AGN.

5. Attachments (Figures)

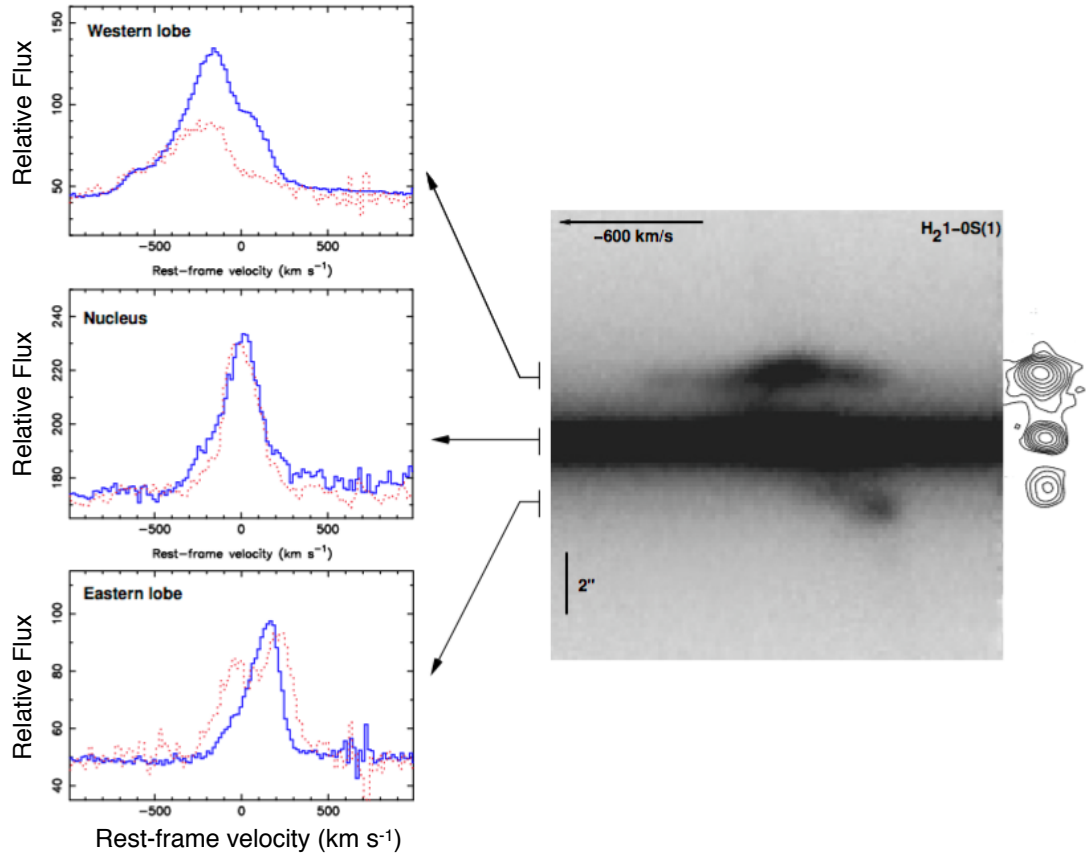


Fig. 3 Evidence of extreme molecular and ionised gas kinematics associated with the radio lobes of the radio AGN IC5063 (from Tadhunter et al. 2014). The greyscale image shows the resolved near-IR long-slit spectrum of the galaxy, aligned along the lobe axis and centred on the $\text{H}_21\text{-}0\text{S}(1)$ line. For comparison, a scaled version of the 1.4 GHz radio map of IC5063 is shown to the right. The velocity profiles derived from spectra extracted from three spatial locations across the galaxy are presented to the left, where the solid blue lines represent the $\text{H}_21\text{-}0\text{S}(1)$ feature, and the dotted red lines represent the $\text{Br}\gamma$ feature. There is clear evidence of highly disturbed, outflowing molecular and ionised gas within the radio lobe, strongly suggesting that the lobe is interacting with the ambient gas of the host galaxy.

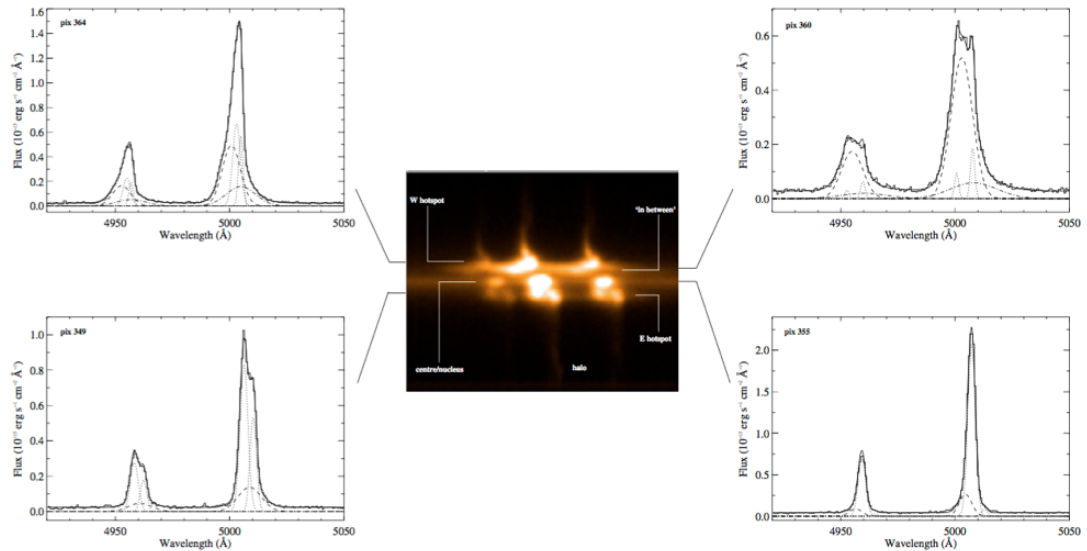


Fig. 4 Evidence of spatially extended ionised outflows measured from the $[\text{O III}]\text{5007}$ line in the radio AGN IC5063 (from Morganti et al. 2007). The central panel shows the 2D long-slit spectrum centred on the $[\text{O III}]\text{5007}$ line. There is significant kinematic complexity in the spatial (i.e., up/down) dimension. Our observations will map these kinematics in all of our sample, identifying extended outflows and establishing their driving mechanism.

6. Experience of applicants with instruments, data quality assessment, data reduction and data product delivery

The members of our team have extensive experience using the VLT and, in particular, its IFUs. Together, we have reduced and published data from KMOS, MUSE, VIMOS, and SINFONI representing over 100 hours of observations. A significant proportion of the KMOS data was taken as part of an ongoing Guaranteed Time Project (led by co-I D. M. Alexander). The first results from this GT program have already been published (Harrison et al. 2016, 2017) and the first results of the analyses have been uploaded to the VizieR database. We note that members of our team (Santoro, Morganti) were awarded Science Verification time on MUSE; the resulting data has already been fully reduced, analysed and published (Santoro et al. 2015ab, 2016). For the proposed MUSE observations, we have allocated a team with extensive experience of ESO pipelines and IFU data reduction (Harrison, Mullaney, Rose, Santoro) to perform an initial reduction within 24 hours of being notified of the completion of each OB. The data will be reduced using the standard ESO pipeline on a dedicated 52-core, 256 GB RAM machine with off-site backup. Since each OB contains three exposures, we will immediately be able to check for spurious outliers within each OB. Furthermore, as each OB represents a third of all data to be taken on each object, there will be sufficient signal per OB to check whether the desired data quality has been obtained, including seeing, signal-to-noise, and photometric reliability. As such, we have the capacity to notify the support staff of any problems with the data before significant amounts of further observations are made. After the initial checks have been completed, we will perform at least two full independent data reductions for each OB; one based at Sheffield (Mullaney, Rose), and another based either at ESO (Harrison) or ASTRON (Santoro). Rose, Harrison and Santoro, in particular, have significant experience manipulating the ESO data reduction pipeline to optimise outputs, so each reduction will be truly independent. Thus, we will be able to perform consistency checks and select the optimum output prior to submission to the archive. As well as reduced datacubes, we will also submit the results of our analyses to the ESO archive. These analysis products will include the results extracted from fitting the stellar continuum and the emission line profiles. Finally, the PI has a track record of making his analysis scripts public, a legacy that will continue with this program, facilitating reproducibility checks and the easy analysis of the public datacubes by others.

7. Data product delivery plan and the team’s resources, e.g., computing facilities, research assistants, etc.

We have allocated a team of four full-time staff and PDRA’s to data reduction, all of whom have significant experience with using the ESO data reduction pipeline to reduce IFU data. In terms of computing resources, the PI’s group has access to a dedicated 52-core, 256 GB RAM machine for data reduction. Data analysis will cover stellar continuum and emission line fitting across the IFU. This analysis will be carried-out using publicly available software (e.g., pPXF, Cappellari & Emsellem 2004), as well as our own in-house IDL and Python software. Reduced (but not analysed) data from each semester will be published within six months of the end of that semester. As well as the reduced data, the PI will ensure that all results of this data analyses are published to the ESO archives within two years of the completed program. Furthermore, all in-house software used to conduct these analyses will be made publicly available. This will enable others to both check our results and easily perform their own analyses using alternative input parameters or on, for example, other emission lines not analysed by default. In what follows, we highlight the tasks that each member of the team has been allocated in order to ensure that all steps in the data reduction, analyses and science publication are carried-out within the required four-year timeframe (two years’ of observations + two years of analyses and science publications):

Data quality assessment: Mullaney (S), Harrison (F), Rose (P), Santoro (D)
Data reduction: Mullaney (S), Harrison (F), Rose (P) , Santoro (D)
Data analyses (i.e., spectral fitting etc): Mullaney (S), Harrison (F), Rosario (F), Rose (P), Spence (D)
Host galaxy and kinematics: Tadhunter (S), Ramos-Almeida (S), Bessiere (F), Dicken (S), Bernhard (P)
Radio Jet/Outflows: Mullaney (S), Tadhunter (S), Morganti (S), Santoro (D), Spence (D)
Outflow properties: Alexander (S), Harrison (F), Villar-Martin (S), Rose (P), Tadhunter (S)
Outflow/host interaction: Mullaney (S), Alexander (S), Harrison (F), Rosario (F), Villar-Martin (S), Bessiere (F)

Key: S = Staff; F = Research Fellow; P = PDRA; D = Doctoral Student

8. Special remarks:

This is a resubmission of a P100 LP proposal. In that previous proposal, we requested observations of the full Southern (unbeamed) 2 Jy sample of 46 AGNs spanning a redshift range $0.05 < z < 0.7$. However, while considering the science case “strong and convincing”, the panel raised concerns regarding the loss of linear resolution in the more distant targets. Acknowledging these concerns, we now restrict the request to target only the $z < 0.4$ AGNs to ensure that we can reach our science goals for the entire sample, thus maximising science output per observing-hour. On the request of the OPC, we now also provide the redshifts and radio luminosities of all our targets (see Box 12). To address another of the OPC’s comments: we stress that there is no better studied sample of radio luminous AGNs *in the whole sky* than the 2 Jy sample. It is therefore the optimal sample for determining the causes and effects of radio AGNs.

9. Justification of requested observing time and observing conditions

Lunar Phase Justification: Since measuring the stellar kinematics and outflow properties (via [O III] λ 5007) relies on the detection of features in the bluer region of the MUSE spectrum, we require dark or grey skies.

Time Justification: (including seeing overhead) The integration time per target is dictated by the need to obtain sufficiently high signal-to-noise in both the stellar continuum and [O III] λ 5007 emission line to map their kinematics to at least one effective radii (~ 10 kpc). This physical extent is needed to (a) ensure that any measured stellar kinematics provide a good representation of the whole galaxy, not just the (possibly decoupled) core and (b) measure the full sphere of influence of any outflows and assess their impact on a significant fraction of the host. Based on previous experience, this demands a signal-to-noise per spectral bin of at least 10 in the continuum. From our own optical imaging campaigns of the 2 Jy sample, the v-band surface brightness of the host at one effective radii is typically $\sim 24^{\text{th}}$ mag arcsec $^{-2}$ (Vega mags.). To obtain a S/N of 10 per pixel at this surface brightness will require unfeasibly long integration times. However, we will adaptively spatially bin to obtain the desired S/N. Entering this surface brightness into the MUSE ETC, adopting an elliptical spectral template, three days from new moon, 1.0'' seeing (to sufficiently resolve the hosts of all AGNs in our sample) and a 2-pixel spectral binning results in a S/N of 1.5 per pixel with 2.5-hours on-target. Binning 6×6 pixels will achieve a S/N of ~ 10 , without a significant loss of spatial resolution beyond the requested 1.0'' seeing. We will split each 2.5-hour on-target observation into twelve 750s DITs, with four DITs per OB (50 mins per OB). Following the MUSE instrument guidelines on overheads, we allocate 12 min per OB to overheads (pointing, acquisition, readout, etc.), resulting in 62 mins per OB. One of our sample has already been observed with MUSE for 1hr 20min, and therefore requires just two OBs. With three OBs for the remaining 35 targets, this gives a total time request of 110.6 hours, distributed over four semesters.

9a. Calibration Request:

Standard Calibration

10. Report on the use of ESO facilities during the last 2 years

KMOS; 095.A-748; 096.A-200; 097.A-0182; 098.A-311 Ongoing GTO program to measure the dynamics, star formation, outflows etc. of star-forming galaxies and AGN. First papers: *Stott et al. (2016); Harrison et al. (2016b, 2017); Magdis et al. (2016); Tiley et al. (2016); Swinbank et al. 2017.*

ALMA; 2016.1.00735.S "Spatially-resolved star formation at high-z; are AGN host galaxies special?". Observations open.

SINFONI; 096.A-600 "AO/IFU observations of a representative sample of $z \approx 1.5$ AGN: what influence do AGN have on their host galaxies?"; Observations carried over, 50% completed.

VIMOS; 099.B-0793. "Quasars "Blowing Bubbles": the impact of AGN on host galaxies", in queue.

11. Applicant's publications related to the subject of this application during the last 2 years

Harrison, C. M., 2017b, Nature Astronomy, arXiv:1703.06889, Invited Review: *Impact of supermassive black hole growth on star formation*

Harrison, C. M., et al. 2017a, MNRAS, 467, 1965, "The KMOS Redshift One Spectroscopic Survey (KROSS): rotational velocities and angular momentum of $z \approx 0.9$ galaxies"

Morganti et al. 2016, A&A, 593, 30: *Another piece of the puzzle: The fast H I outflow in Mrk 231*

Morganti et al. 2016, A&A, 592, 94: *Missing link: Tracing molecular gas in the outer filament of Centaurus A*
Johnson, Harrison et al. 2016, MNRAS, 460, 1059: *The spatially resolved dynamics of dusty starburst galaxies in a $z \approx 0.4$ cluster: beginning the transition from spirals to S0s*

Villar-Martin et al. 2016, MNRAS, 460, 130: *Ionized outflows in luminous type 2 AGNs at $z \approx 0.6$: no evidence for significant impact on the host galaxies*

Spence et al. 2016, MNRAS, 459, 16: *No evidence for large-scale outflows in the extended ionized halo of ULIRG Mrk273*

Tadhunter 2016, A&AR, 24, 10: *Radio AGN in the local universe: unification, triggering and evolution*

Santoro et al. 2016, A&A, 590, 37S: *Embedded star formation in the extended narrow line region of Centaurus A: Extreme mixing observed by MUSE*

Villar-Martin et al. 2015, MNRAS, 454, 419: *Deconstructing the narrow-line region of the nearest obscured quasar*

Morganti et al. 2015, A&A, 580, 1: *The fast molecular outflow in the Seyfert galaxy IC 5063 as seen by ALMA*

Santoro et al. 2015, A&A, 575, 4: *The outer filament of Centaurus A as seen by MUSE*

Harrison et al. 2015, ApJ, 800, 45: *Storm in a "Teacup": A Radio-quiet Quasar with 10 kpc Radio-emitting Bubbles and Extreme Gas Kinematics*

Santoro et al. 2015, A&A, 574, 89: *The jet-ISM interaction in the outer filament of Centaurus A*

Tadhunter et al. 2014, MNRAS, 445, 51: *The dust masses of powerful radio galaxies: clues to the triggering of their activity*

12. List of targets proposed in this programme

Run	Target/Field	α (J2000)	δ (J2000)	ToT	Mag.	Diam.	Additional info	Reference star
A	PKS0034-01	00 37 04.1	-01 09 08.2	3.1	25.3		z=0.07	
A	PKS0043-42	00 46 17.8	-42 07 51.4	3.1	26.0		z=0.12	
A	PKS1934-63	19 39 25.0	-63 42 45.6	2.1	26.8		z=0.18	
A	PKS2356-61	23 59 04.5	-60 54 59.1	3.1	26.0		z=0.10	
A	PKS1839-48	18 43 14.6	-48 36 23.3	3.1	25.6		z=0.11	
A	PKS1733-56	17 37 35.8	-56 34 03.4	3.1	25.9		z=0.10	
A	PKS2250-41	22 53 03.2	-40 57 46.2	3.1	26.6		z=0.31	
A	PKS2211-17	22 14 25.8	-17 01 36.2	3.1	26.1		z=0.15	
A	PKS0038+09	00 40 50.5	+10 03 26.8	3.1	26.2		z=0.19	
A	PKS2135-14	21 37 45.2	-14 32 55.5	3.1	26.2		z=0.20	
A	PKS1949+02	19 52 15.8	+02 30 23.1	3.1	25.3		z=0.06	
B	PKS0347+05	03 49 46.5	+05 51 42.3	3.1	26.7		z=0.34	
B	PKS0404+03	04 07 16.5	+03 42 25.8	3.1	25.7		z=0.09	
B	PKS0442-28	04 44 37.7	-28 09 54.6	3.1	26.1		z=0.15	
B	PKS0625-35	06 27 06.7	-35 29 16.3	3.1	25.2		z=0.05	
B	PKS0806-10	08 08 53.6	-10 27 40.2	3.1	25.7		z=0.11	
B	PKS0915-11	09 18 05.7	-12 05 44.0	3.1	26.0		z=0.05	
B	PKS0620-52	06 21 43.3	-52 41 33.3	3.1	24.9		z=0.05	
C	PKS1559+02	16 02 27.4	+01 57 55.7	3.1	25.9		z=0.10	
C	PKS0035-02	00 38 20.5	-02 07 40.1	3.1	26.2		z=0.22	
C	PKS0039-44	00 42 09.0	-44 14 01.3	3.1	26.7		z=0.35	
C	PKS1355-41	13 59 00.2	-41 52 54.1	3.1	26.7		z=0.31	
C	PKS0023-26	00 25 49.2	-26 02 12.8	3.1	27.0		z=0.32	
C	PKS1648+05	16 51 08.2	+04 59 33.8	3.1	26.9		z=0.15	
C	PKS1814-63	18 19 35.0	-63 45 48.1	3.1	25.5		z=0.06	
C	PKS1932-46	19 35 56.6	-46 20 40.7	3.1	26.7		z=0.23	
C	PKS1954-55	19 58 16.1	-55 09 37.5	3.1	25.1		z=0.06	
C	PKS2221-02	22 23 49.6	-02 06 12.4	3.1	25.2		z=0.06	
C	PKS2314+03	23 16 35.2	+04 05 18.2	3.1	26.3		z=0.22	
D	PKS1151-34	11 54 21.8	-35 05 29.1	3.1	26.7		z=0.26	
D	PKS0945+07	09 47 45.2	+07 25 20.4	3.1	25.7		z=0.09	
D	PKS0105-16	01 08 16.9	-16 04 20.6	3.1	26.8		z=0.40	
D	PKS0859-25	09 01 47.5	-25 55 19.0	3.1	26.7		z=0.31	
D	PKS0349-27	03 51 35.8	-27 44 33.8	3.1	25.3		z=0.07	
D	PKS0625-53	06 26 20.4	-53 41 35.2	3.1	25.0		z=0.05	

Following targets moved to the end of the document ...

Target Notes: The “Mag.” column contains the \log_{10} rest-frame 5 GHz radio luminosity of the target in units of W Hz^{-1} .

12a. ESO Archive - Are the data requested by this proposal in the ESO Archive (<http://archive.eso.org>)? If so, explain the need for new data.

One of our targets, PKS1934-063 has been observed by MUSE for a total of 1hr20 minutes. This data is not, however, deep enough to reach our primary science goals. We therefore request a further 100 mins observing time on this single object (to fit within our OB structure).

12b. GTO/Public Survey Duplications:

There is no duplication of the requested targets in ongoing GTO programmes.

13. Scheduling requirements

14. Instrument configuration

Period	Instrument	Run ID	Parameter	Value or list
--------	------------	--------	-----------	---------------

4b. Co-investigators:

...continued from Box 4a.

R.	Morganti	1096
C.	Ramos-Almeida	1393
D.	Rosario	1237
M.	Rose	1245
F.	Santoro	1096
R.	Spence	1245
M.	Villar-Martin	8545

12c. List of targets proposed in this programme

Run	Target/Field	α (J2000)	δ (J2000)	ToT	Mag.	Diam.	Additional info	Reference star
-----	--------------	------------------	------------------	-----	------	-------	--------------------	----------------

...continued from box 12.

D	PKS0213-13	02 15 37.5	-12 59 30.5	3.1	26.0		z=0.15	
---	------------	------------	-------------	-----	------	--	--------	--